

SUPPORTING INFORMATION

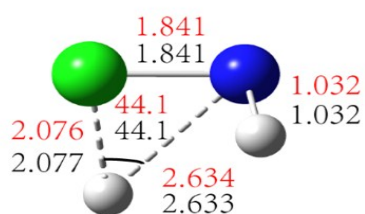
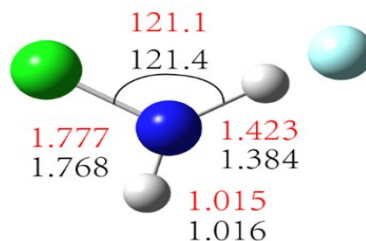
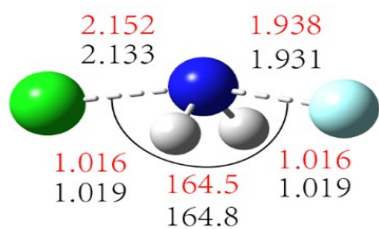
New Proposed Proton-abstracted Roundabout with Backside Attack Mechanism for the S_N2 Reaction at Nitrogen Center $F^- +$ NH_2Cl

Yongfang Li and Dunyou Wang^{†}*

College of Physics and Electronics, Shandong Normal University, Jinan Shandong
250014, China

^{*}Author to whom correspondence should be addressed. Email: dywang@sdnu.edu.cn

CCSD(T)/aug-cc-pVTZ
DFT/M06-2X/aug-cc-pVDZ



CCSD(T)/aug-cc-pVTZ
DFT/M06-2X/aug-cc-pVDZ

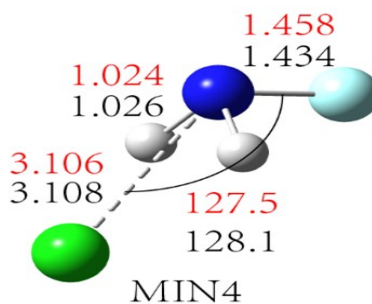
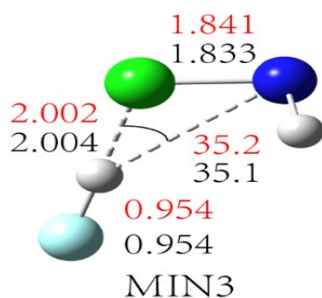
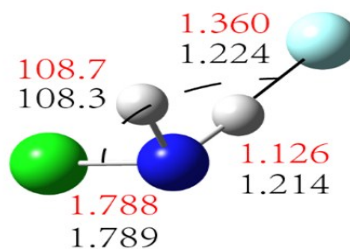
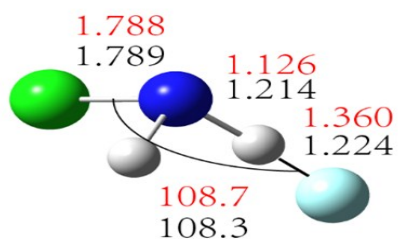


Figure.S1 Comparison of geometries of the stationary points (in Å and degrees) between the DFT/M06-2X/aug-cc-pVDZ and CCSD(T)/aug-cc-pVTZ levels of theory

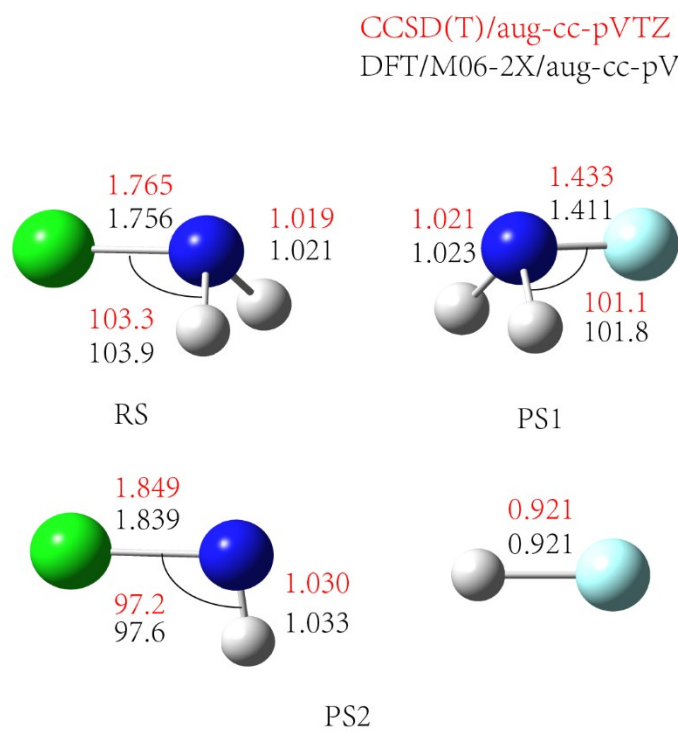


Figure S2. Comparison of gemoetries of the reactants and products (in Å and degrees) between DFT/M06-2X/aug-cc-pVDZ and CCSD(T)/aug-cc-pVTZ levels of theory.

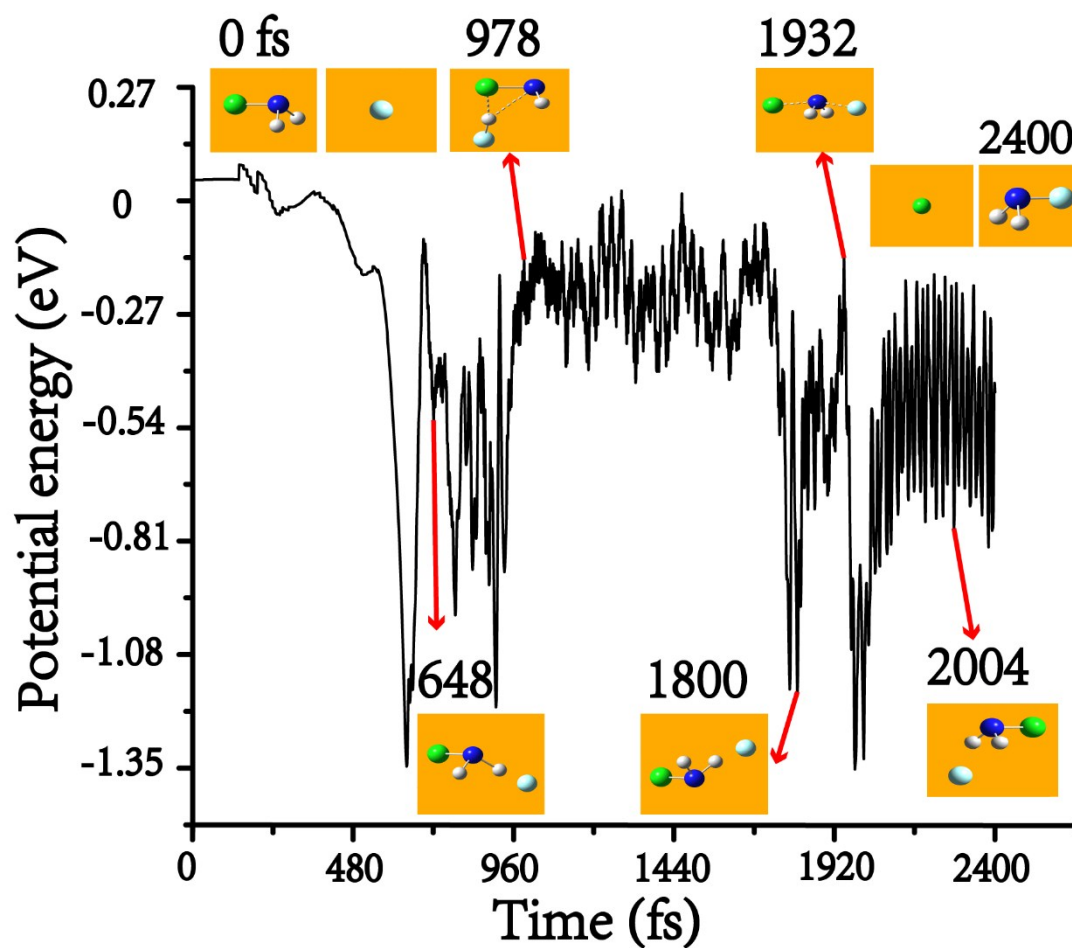


Figure S3. Potential energy vs. time from another PAR&BAR reactive trajectory. The labelled points along the reactive trajectory are used to search and locate the stationary points of the PAR&BAR potential energy profile in Figure 4, leading to the stationary points: RS, MIN1, TS3, MIN2, TS1, MIN4 and PS1, respectively.

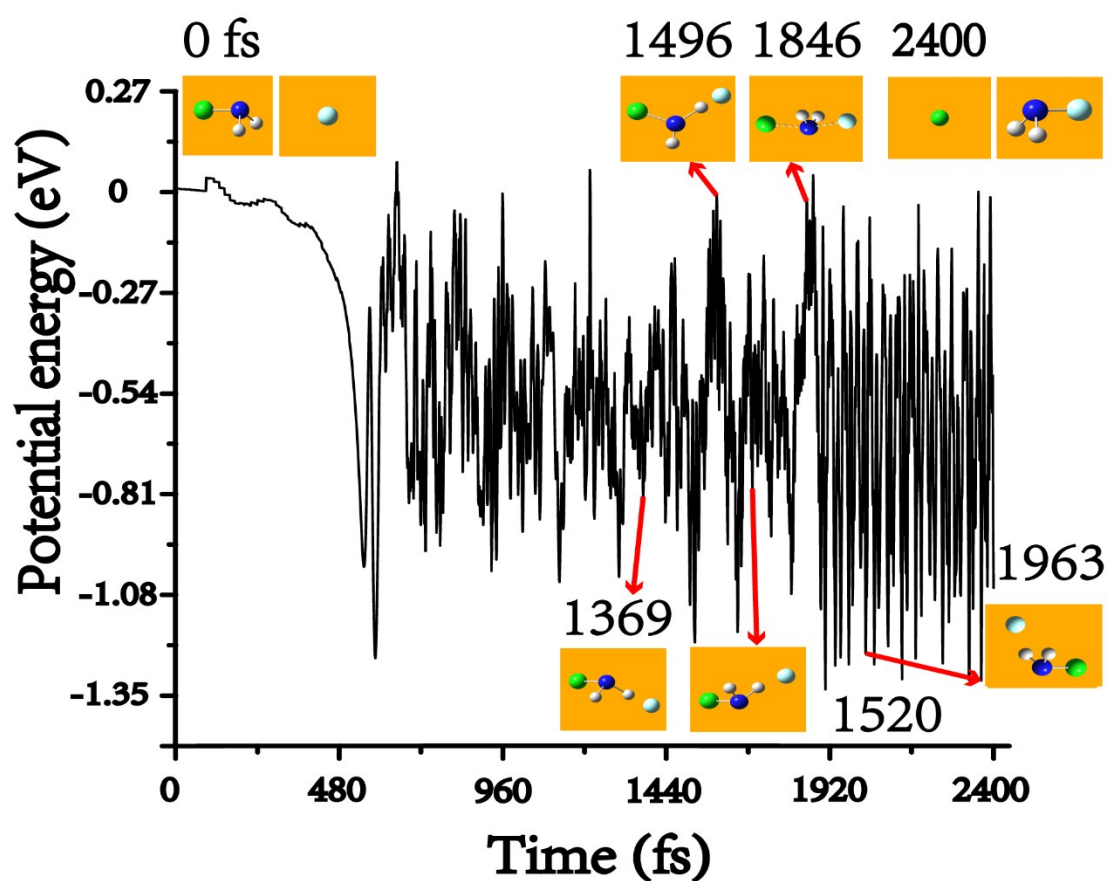


Figure S4. Potential energy vs. time from a double-inversion reactive trajectory. The labelled points along the reactive trajectory are used to search and locate the stationary points of the double-inversion potential energy profile in Figure 4, leading to the stationary points: RS, MIN1, TS2, MIN2, TS1, MIN4 and PS1, respectively.

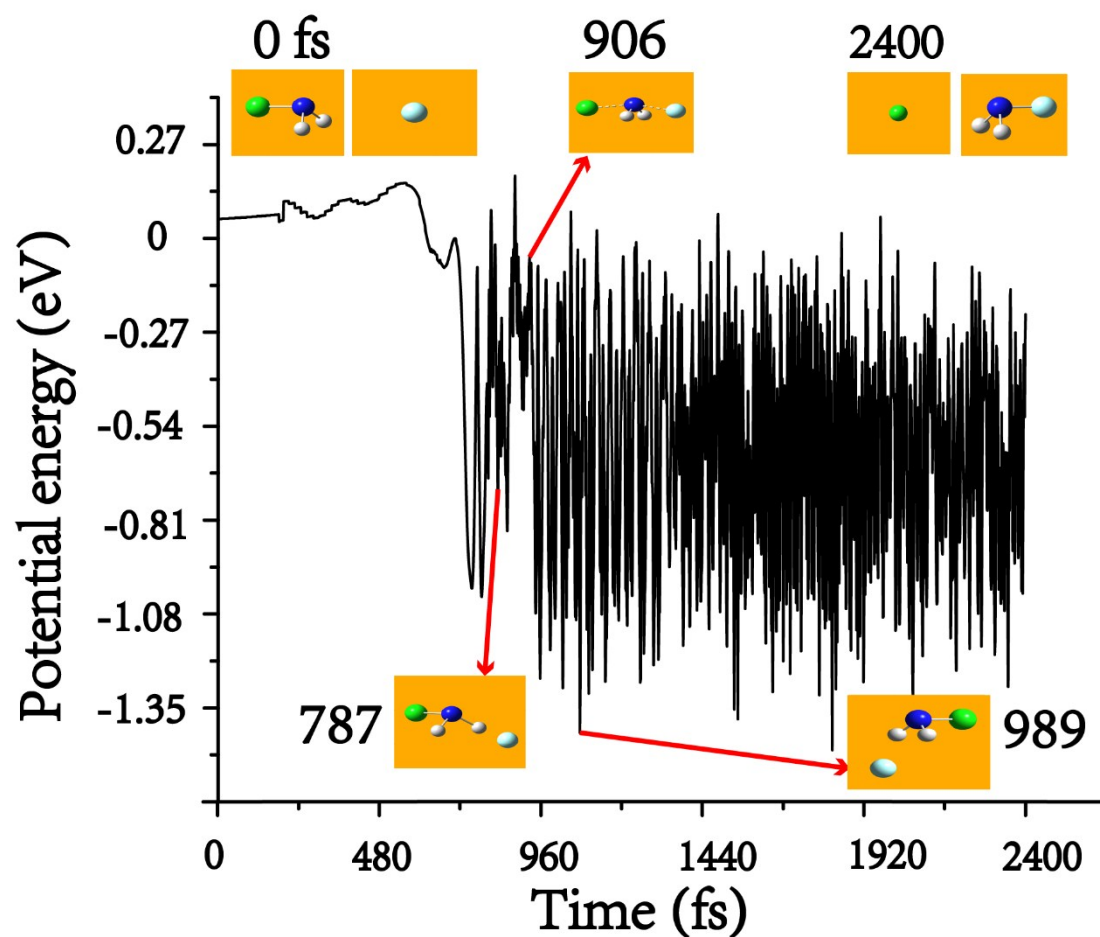


Figure S5. Potential energy vs. time from a hydrogen-bond mechanism reactive trajectory. The labelled points along the reactive trajectory are used to search and locate the stationary points of the hydrogen-bond potential energy profile in Figure 4, leading to the stationary points: RS, MIN1, TS1, MIN4 and PS1, respectively.

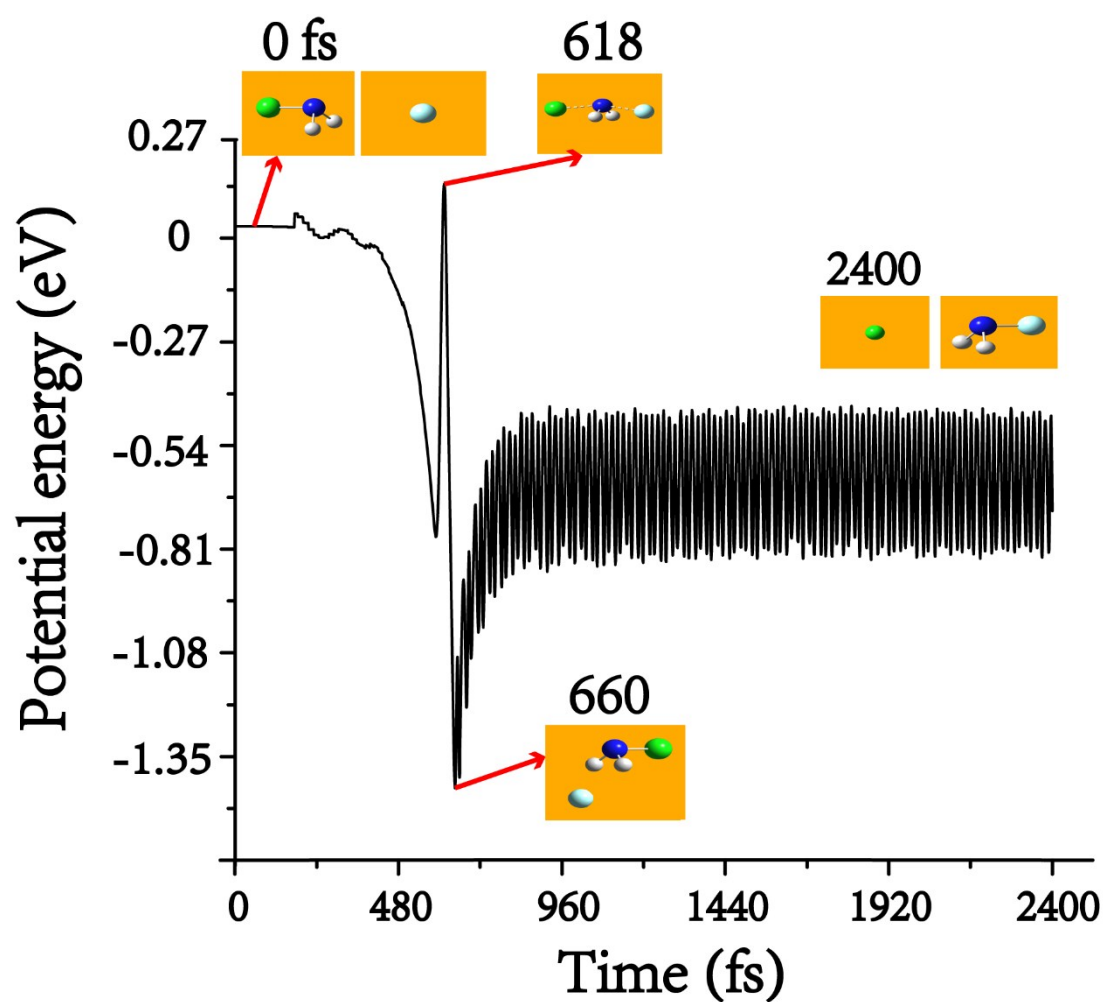


Figure S6. Potential energy vs. time from a direct rebound reactive trajectory. The labelled points along this reactive trajectory are used to search and locate the stationary points of the potential energy profile in Figure 4, leading to the stationary points: RS, TS1, MIN4 and PS1, respectively.

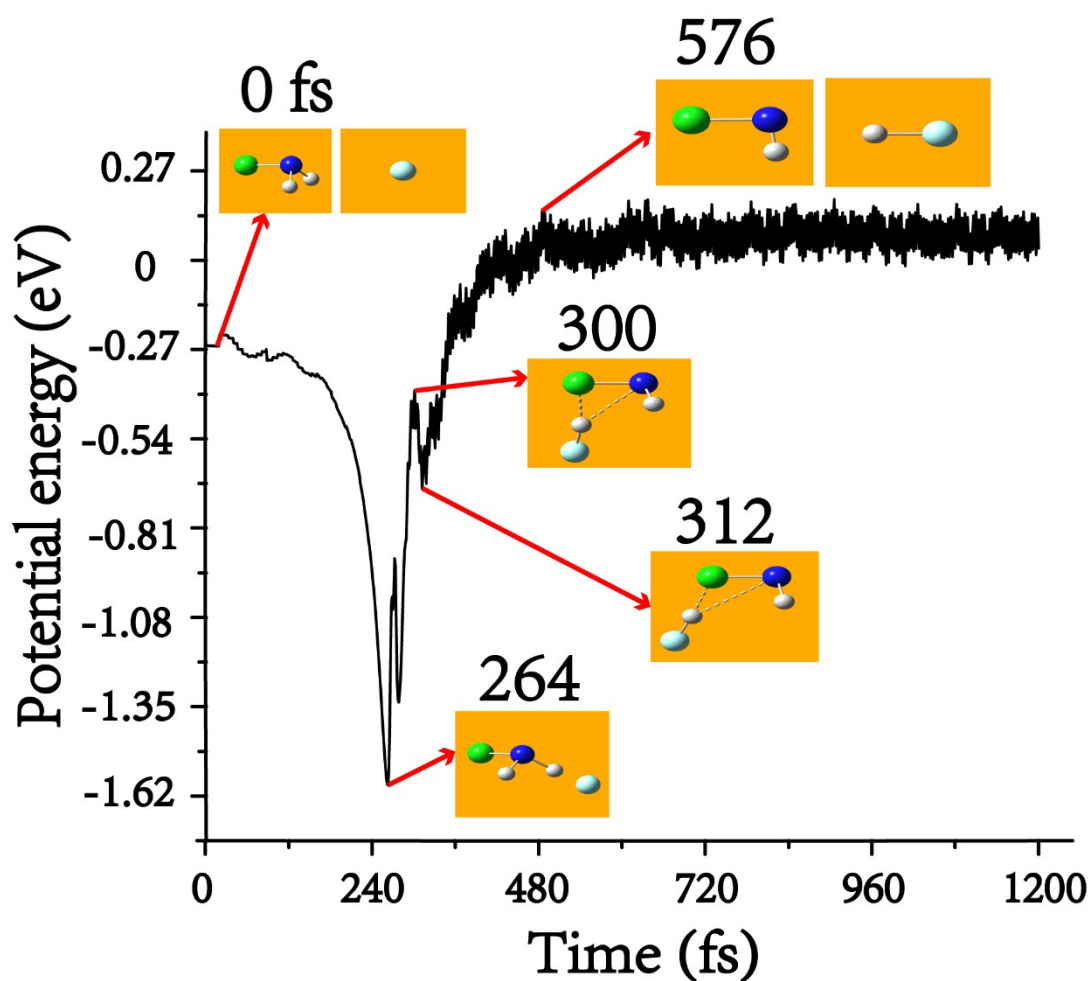


Figure S7. Potential energy vs. time from an abstraction reactive trajectory. The labelled points along this reactive trajectory are used to search and locate the stationary points of the abstraction potential energy profile in Figure 4, leading to the stationary points: RS, MIN1, TS3, MIN3 and PS2, respectively.

Table S1. Relative energies in kcal/mol of stationary points from our DFT/aug-cc-pVDZ and CCSD(T)-F12/aug-cc-pVTZ results and the benchmark results at the CCSD(T)-F12b/aug-cc-pV5Z(-PP) level of theory^a.

	DFT/aug-cc-pVDZ	CCSD(T)-F12/aug-cc-pVTZ ^b	CCSD(T)-F12b/aug-cc-pV5Z(-PP)
RS ($\text{F}^- + \text{NH}_2\text{Cl}$)	0.0	0.0	0.0
MIN1	-33.1	-30.6	-30.2
MIN2	-33.1	-30.6	-30.0
MIN3	-12.6	-10.5	-10.2
MIN4	-36.5	-30.0	-29.6
TS1	-14.2	-12.5	-11.9
TS2	-27.4	-23.7	NA
TS3	-12.4	-10.1	-9.7
PS1 ($\text{Cl}^- + \text{NH}_2\text{F}$)	-20.3	-14.0	-13.6
PS2 ($\text{HF} + \text{NHCl}^-$)	5.3	7.1	7.3

- a. From Ref. 41. Benchmark classical relative energies obtained as CCSD(T)-F12b/aug-cc-pV5Z(-PP) with core correlation effects.

Table S2. Cartesian coordinates(\AA) of the stationary points at the CCSD(T)/aug-cc-pVTZ level of theory.

RS (NH₂Cl)

H	-0.938	0.005	1.391
H	0.465	0.815	1.391
N	0.044	-0.077	1.133
Cl	0.009	-0.016	-0.630

MIN1

H	1.036	0.011	0.224
H	0.037	-1.128	0.961
N	0.083	-0.119	0.809
Cl	-1.230	0.089	-0.386
F	2.262	0.068	-0.363

MIN2

H	1.036	0.011	-0.224
H	0.037	-1.128	-0.961
N	0.083	-0.119	-0.809
Cl	-1.230	0.089	0.386
F	2.262	0.068	0.363

MIN3

H	0.137	1.301	0.042
H	-1.384	-1.556	0.417
N	-0.692	-1.629	-0.342
Cl	0.619	-0.600	0.442
F	-0.029	2.231	-0.091

MIN4

H	-0.578	-0.775	-0.291
H	-0.581	0.777	-0.292
N	-1.247	0.000	-0.301
Cl	1.667	-0.002	0.774
F	-1.680	-0.001	-1.693

TS1

H	-0.227	-0.802	-0.632
H	-0.216	0.792	-0.657
N	-0.518	0.006	-0.088
Cl	1.377	0.009	0.931
F	-1.917	-0.006	-1.429

TS2

H	-1.692	-0.270	-0.794
H	-0.216	1.282	-0.054
N	-0.815	0.034	-0.384
Cl	0.033	-1.498	-0.078
F	0.186	2.205	0.173

TS3

H	0.674	0.790	0.709
H	0.254	-2.076	0.145
N	-0.542	-1.540	0.527
Cl	-0.514	-0.167	-0.700
F	1.239	1.346	1.225

PS1 (NH₂F)

H	-0.922	-0.022	0.933
H	0.480	0.787	0.934
N	0.065	-0.112	0.684
F	0.000	0.000	-0.742

PS2 (NHCl⁻)

N	1.6276	-1.866	-0.560
H	1.391	-0.863	-0.560
Cl	3.465	-1.673	-0.560

PS2 (HF)

F	3.213	0.637	0.000
H	2.292	0.637	0.000

Table S3. Harmonic vibrational frequencies (cm⁻¹) for the stationary points at the CCSD(T)-F12/aug-cc-pVTZ level of theory.

	MIN1	MIN2	MIN3	MIN4	TS1	TS2	TS3
ZPE	5598.7	5598.7	5256.8	6156.1	5528.3	4897.9	5144.5
1	130.8	130.8	80.4	53.2	422.7 <i>i</i>	441.6 <i>i</i>	108.4 <i>i</i>
2	393.9	393.9	166.7	113.0	235.2	115.3	186.9
3	511.2	511.2	213.5	164.4	260.1	340.3	250.6
4	615.9	615.9	507.4	857.6	317.9	664.8	516.9
5	1212.9	1212.9	776.5	1303.8	969.4	1067.9	585.0
6	1411.2	1411.2	812.5	1362.2	1067.3	1221.6	736.9
7	1597.7	1597.7	1244.7	1584.2	1530.9	1354.7	1246.0
8	1890.0	1890.0	3313.0	3414.2	3498.9	1964.2	3287.1
9	3434.3	3434.3	3398.8	3459.5	3599.5	3508.5	3588.0

	RS (NH ₂ Cl)	PS1 (NH ₂ F)	PS2 (NHCl ⁻)	PS2 (HF)
ZPE	5765.9	6032.8	2521.4	2045.6
1	670.8	918.6	511.7	4091.2
2	1092.5	1276.7	1227.8	
3	1196.7	1346.3	3303.3	
4	1604.0	1628.5		
5	3436.6	3399.2		
6	3531.2	3496.3		